ORGANIZATION FOR NUCLEAR RESEARCH

PARTON INTERPRETATION OF LOW P_T DEEP INELASTIC PROTON-PROTON COLLISIONS AT $s = 2000\ GeV^2$

F. C. Erné and J. C. Sens
Foundation for Fundamental Research on Matter, The Netherlands
and
CERN, Geneva, Switzerland

Abstract

Data on the inclusive production of low p_T, high x pions and kaons are compared with several current parametrizations of the parton model. There is consistency with the view that fast mesons are produced through the combination of a fast valence quark with a slow sea quark in one of the colliding protons. The pion data are compatible with substantial production of ρ-mesons. Sumrules and the Drell-Yan dimuonspectra are discussed.

Geneva - January 1978
(Submitted to Physical Review Letters)

With the advent of data, first [1] at $p_{eq.lab} \simeq 1000$ GeV (CERN/ISR) and recently also [2] at $p_{lab} = 100$, 200 and 400 GeV (FNAL) on $pp \to \pi^{\pm}X$, $pp \to K^{\pm}X$, where the produced $\pi^{\pm}$, $K^{\pm}$ have high fractional longitudinal momentum $x(= 2p_L/\sqrt{s})$ and small transverse momentum, it has become apparent[3] that deep inelastic pp collisions in which a large fraction of the available energy is carried off by a single secondary provide information on the constituent structure of the proton, complementary to that obtained in deep inelastic electron and neutrino scattering and in the production of lepton pairs. In such collisions the momentum distribution of a fast emerging meson is, in first instance, expected to resemble the high momentum tail of the parent valence quark distribution in the proton. Although this simple picture is in qualitative agreement with data [1,2], it has recently been pointed out by Das and Hwa [4] that the recombination of an antiquark $\bar{q}$ from the sea with a valence quark q should rather strongly modify the momentum distribution of the meson. In ref.4 a comparison is made between this assertion and a limited selection of the data of ref.1. As pointed out by Pokorski and Van Hove [5] this comparison is complicated by the fact that a fraction of the produced mesons may result from the decay of low mass resonances and hence that the correspondence between the observed mesons and the quark flavours in the proton is not unique.

In the following we compare the complete set of data of ref.1 with the Das and Hwa model. We shall show that the data can indeed be understood in terms of the $q\bar{q}$ recombination mechanism and current parametrizations of the distributions q(x) of the various flavours, but that, in the absence of data on the production of low mass resonances at high x and low p_T, a certain trade-off between the parametrizations involved in $q\bar{q}$-recombination and resonance production can not be excluded.

Following Das and Hwa [4] we write the invariant differential cross-section for the inclusive direct production of a meson with fractional momentum x and transverse momentum p_T as :

$$E\frac{d^3\sigma}{dp^3} \equiv C(q_iq_j,x) = A(p_T^2)\frac{1-x}{x}\int_0^x dx_1\int_0^x dx_2\; x_1x_2q_i(x_1)q_j(x_2)\delta(x-x_1-x_2) \qquad (1)$$

./.

Here $q_k(x)$ are the momentum distributions of the flavours k = u,d,s and the delta function reflects the assumed two-constituent character of the meson production process. The factors in front of the convolution integral arise from phase space and the explicitly inserted p_T dependence of the data. The factorization in p_T and x is in accord with the observed absence of correlation between p_T and x for x > 0.5 in the data [1].

For low mass $q\bar{q}$ resonance production and subsequent isotropic decay into a meson with fractional momentum x we have to a good approximation :

$$E\frac{d^3\sigma}{dp^3} = x\int_x^1 \frac{C(q\bar{q}, x_R)\, dx_R}{x_R^2} \qquad (2)$$

where x_R is the fractional momentum of the resonance; the smearing in the p_T distributions due to the decay has been ignored.

For the momentum distributions q(x), $\bar{q}(x)$ we have $\pi^+ = u\bar{d}$, $\pi^- = d\bar{u}$, $K^+ = u\bar{s}$, $K^- = s\bar{u}$. For q(x) we use three parametrizations, one due to Blankenbecler et al. [6] (I), one due to Dao et al. [7] (II) and one due to Field and Feynman [8] (III). The three sets of q(x) are all based on deep inelastic electron scattering data. In II these data have been combined with recent μ-pair production data [9] at 400 GeV and $5 < m_{\mu\mu} < 15$ GeV to deduce the valence distributions $u_v(x)$, $d_v(x)$ and the sea distributions $u_s = \bar{u}_s = d_s = \bar{d}_s = s_s = \bar{s}_s \equiv s(x)$. In III they have been combined with neutrino data, particle production data at high p_T and theoretical input to deduce the various q(x). In particular it is found that $xu(x) \sim (1-x)^3$, $xd(x) \sim (1-x)^4$; $xu_s(x) \sim (1-x)^{10}$, $xd_s(x) \sim (1-x)^7$, $xs_s(x) = x\bar{s}_s(x) \sim (1-x)^8$ are in best agreement with most available data.

As a first step we compare the data with eq.(1) for the parametrizations I, II and III with all parameters fixed, i.e. as derived by the authors of ref. 6,7,8 resp., and assuming all mesons to be produced directly, without resonance production. Only the factors $A(p_T^2)$ of eq.(1) are adjusted to the data. Fig.1 show the data at $p_T = 0.75$ GeV compared with parametrization III; the curves labeled $C(q\bar{q},x)$ indicate the convoluted $q\bar{q}$ distributions of eq.(1). For comparison the 'bare' distributions $\pi^+(x) = u(x)$ etc. computed with the same parametrizations III are also indicated.

./.

Inspection of fig.1 reveals the following features :

1) the convoluted distributions (eq.(1)), in the parametrization of Field and Feynman (III), are in good agreement with the data on π^-, K^+ and K^-; for π^+ there are significant deviations at $x \gtrsim 0.85$;

2) association of the momentum of the produced fast meson with that of the valence quark of the appropriate flavour is in disagreement with the data;

3) the K^- data constitute a measure of the sea quark momentum distributions only; comparison with the convoluted distribution $C(s\bar{u},x)$ indicates that the parametrizations of the $s(x)$ and $\bar{u}(x)$ distributions as somewhat arbitrarily chosen in III are consistent with the data.

In the parametrizations I and II, both the bare flavour momentum distributions $q(x)$ and the convoluted distributions $C(q\bar{q},x)$ resemble those of III; in particular the disagreement between $C(u\bar{d},x)$ and the π^+ distributions persists. The spectra for model II are shown in fig.2.

In order to understand the origin of the disgreement in the π^+ spectra we have updated models II and III (and discarded model I; it is based on less data than II and III). As mentioned above model II is based on a combination of high mass μ-pair production [9] and ep-scattering data. In a recent analysis [10] of the μ-pair continuum data (after correction for the effect of Fermi motion in the target (Pt) nucleus) in terms of the Drell-Yan expression for the annihilation of a $q\bar{q}$ pair good agreement is obtained with a sea parton distribution of the form $x\,s(x) \sim (1-x)^{10}$. We have therefore updated model II (model IIa) using this form for all sea parton flavours and the relations :

$$\nu W_2^p = \frac{4}{9} u_v(x) + \frac{1}{9} d_v(x) + \frac{4}{3} s(x)$$

$$\nu W_2^n = \frac{1}{9} u_v(x) + \frac{4}{9} d_v(x) + \frac{4}{3} s(x) \qquad (3)$$

to compute the valence distributions $u_v(x)$ and $d_v(x)$ using the parametrization of ref.11 for the structure functions at the left side of eq.(3).

./.

The results are shown in fig.2; they shown that the agreement with the π^+ data is improved, while the agreement with the π^+, K^+, K^- data remains satisfactory.

Model III, in which the various sea parton distributions have different x-dependence, has been updated by noting that the π^+-distribution is the only one sensitive to the $\bar{d}(x)$ distribution. An x-dependence of the form $x\bar{d}(x) = 0.15\ (1-x)^{10}$ gives the results (model IIIa) shown in fig.1, in good agreement with experimental π^+ spectra.

The x-distributions at other values of p_T, in the range $0.55<p_T<1.05$ GeV, show the same features as those at $p_T = 0.75$ GeV in fig.1. Figs.3 and 4 show to what extend the data at various p_T are in agreement with model IIIa.

Next we consider to what extent the conclusions concerning the parton content of the high x meson spectra are affected by resonance decay. We note that high mass resonances decaying into several particles result mostly in low x mesons; hence only ρ and K^* decay will be considered here. We retain the recombination mechanism of eq.(1) by generating pions through the recombination of q and $\bar{q}$ partly into direct pions, partly into ρ's followed by decay :

$$\begin{array}{lll} \pi^+ = C(u\bar{d}) & \rho^+ = C(u\bar{d}) \to \pi^+ & \rho^0 = C(\ \tfrac{1}{2}u\bar{u} + \tfrac{1}{2}d\bar{d}\ ) \to \pi^+ \\ \pi^- = C(d\bar{u}) & \rho^- = C(d\bar{u}) \to \pi^- & \rho^0 = C(\ \tfrac{1}{2}u\bar{u} + \tfrac{1}{2}d\bar{d}\ ) \to \pi^- \end{array} \qquad (4)$$

where C, as above, indicates the convolution in eq.(1). Similarly, K-mesons are generated in part directly, in part through $K^* \to K$ decay. The contribution of K^* decay to the pion spectra is ignored. We note that, through ρ^0 decay, the 'wrong' valence quark flavour is fed into the π^+ and π^- spectra, while for K^* there is no such mixing. In view of the equality in flavour content of the charged π's and charged ρ's (only the spins are different) we assume the relative strengh of $\rho\pm$, ρ^0 production to be related by the relations :

$$\frac{\rho^+}{\rho^-} = \frac{\pi^+}{\pi^-} \qquad \rho^0 = \frac{\rho^+ + \rho^-}{2} \qquad (5)$$

./.

leaving 1 extra constant to be determined for the combined π^+ and π^- spectra [12]. The 'direct' and the ρ-decay contributions to the π^+ and π^- spectra calculated with model III are shown in fig.5, along with their sums. A calculation with model II gives a similar result. It appears that the thus computed π^+ spectra are in better agreement with the data while the π^- spectra are not substantially modified. The improvement in the π^+ spectra is similar in magnitude and x-dependence to the improvement obtained by the updated models IIa and IIIa discussed above. We are therefore unable to choose between the two alternatives, faster fall-off with x of all sea parton distributions (model IIa) resp. the down-sea parton distribution (model IIIa), or contributions due to ρ-decay. The computed ρ-decay spectra of fig.5 are thus in the nature of a prediction, and do not replace the need for an experiment specifically designed to measure ρ-decay at high x. Taken at face-value the yield of π^+ with $x > 0.5$ is 23% (18%) ρ-decay-pions and 77% (82%) 'direct' pions; for π^- the result is 35% (31%) ρ-decay, 65% (69%) 'direct' for model III (II). This result corresponds to a ρ/'direct' ratio of 1.5 (1.1) in the total x-range. The K-meson data appear to be consistent with direct production only, presumably as a result of the similarity in flavour content of K and K^* mentioned above.

In all models the normalizations are taken to be such that the following sumrules are satisfied to within 10% :

$$\begin{aligned} \int(u(x) - \bar{u}(x))dx &= 2 \\ \int(d(x) - \bar{d}(x))dx &= 1 \\ \int(s(x) - \bar{s}(x))dx &= 0 \end{aligned} \tag{6}$$

$$\int_0^1 \left(\nu W_2^p - \nu W_2^n \right) \frac{dx}{x} = \frac{1}{3} + \frac{2}{3} \int_0^1 (\bar{u}(x) - \bar{d}(x))dx = \frac{1}{3} \tag{7}$$

Eq.(7) follows from eq.(3) and eq.(6). We find furthermore that in all models

$$\int x\, u(x)dx = 0.29 \qquad \int x d(x)dx = 0.15 \qquad \int x q_{SEA}(x)dx = 0.01 - 0.025$$

./.

to within ~ 3%, totaling to ~ 50% and leaving 50% of the total momentum unaccounted for by partons.

A constraint to be respected in postulating parton momentum distribution functions is the requirement that the computed Drell-Yan continuum agrees with the high mass μ-pair data, both in magnitude and shape, while, simultaneously, the sumrules of eq.(6) and (7) are satisfied. The μ-pair data of ref.9 are per nucleon in Cu(67%) and Pt(33%) combined and the cross-sections have been computed assuming isotropic decay into 2 muons. The data of ref.10 are per nucleon Pt (60%n, 40%p), based on $1 + \cos^2\theta$ decay, and have been corrected for Fermi motion. The models I, II and III were formulated before the data of ref.10 were available.

We have computed the Drell-Yan continuum per nucleon in Pt for all modules (I, II, IIa, III, IIIa) with the following results. In model I the sumrules are satisfied, but the mass dependence differs strongly from the data of ref.10. Model II has been derived from the (earlier) data of ref.9; it thus agrees with ref.9, it satisfies the sumrules but is ~ 30% below the (corrected) data of ref.10. Renormalizing the sea-distribution s(x), to which the Drell-Yan cross-section at y = 0 is approximately proportional, restores agreement with the data (ref.10) but destroys the agreement with the sumrules. The updated model IIa is, depending on the choice of normalization, either in agreement with ref.10 (by design) or with the sumrules but not with both. Models III and IIIa both satisfy the sumrules but remain substantially below the data of ref.10. We note that the shape of the updated Field-Feynman distribution is in excellent agreement with the high mass μ-pair data of ref.10 but that the normalization differs by a factor of about 3. Generally it appears that no current model simultaneously satisfies the sumrules and the recently obtained μ-pair data. This defect can be remedied (by raising the sea quark normalization constants and altering the x dependence) but not without the penalty of worsening the agreement with the pp → hX data (in particular for $h = K^-$) of this experiment, and of modifying νW_2^p and νW_2^n for $x \lesssim 0.2$. We note that a large part of the integral in the sumrules arises from the region $x < 0.2$ where little data is available and the input to q(x) is largely based on hypothesis. With

./.

these reservations it is nevertheless interesting to observe that removing the color variable from the Drell-Yan expression would restore the agreement between models II and III, the data, the sumrules and the structure functions. In fig. 6 the dimuondata of ref. 10 are compared with the models used in this analysis.

We conclude that the accurate data of ref.1 taken at p^{eq}_{lab} = 1 TeV and extending to x = 0.95 have enabled us to relate deep inelastic proton-proton scattering to deep inelastic electron (muon, neutrino) proton scattering and to lepton pair production through the common underlying mechanism of the parton model and the recombination mechanism for meson production at high momenta. A measurement of the production of low mass resonances, in particular ρ, would resolve some of the ambiguities that remain in the momentum distribution of the different quark flavours. The Drell-Yan distributions computed from these distributions do not simultaneously agree with high mass μ-pair data and the sumrules.

We are indebted to E. Berger for useful comments.

REFERENCES

1. Tables of cross-sections for $pp \to \pi^{\pm} X$, $pp \to K^{\pm} X$ (CHLM collaboration, 1975, unpublished); J. Singh et al., to be published in Nucl.Phys.B.

2. J. R. Johnson et al., PRL 39 (1977) 1173.

3. W. Ochs, Nucl. Phys. B118 (1977) 397.

4. K. P. Das and Rudolph C. Hwa, Oregon University Report No. OITS-73, 1977 (unpublished). The conclusions of the paper are mostly based on comparison with the data of ref.1.

5. S. Pokorski and L. Van Hove, CERN-preprint TH-2427, Nov.1977.

6. R. Blankenbecler et al., SLAC-PUB-1531 (1975).

7. F. T. Dao et al., PRL 39 (1977) 1388.

8. R. D. Field and R. P. Feynman, PR D15 (1977) 2590.

9. S. W. Herb et al., PRL 39 (1977) 252.

10. D. M. Kaplan et al., submitted to PRL.

11. W. B. Atwood, SLAC Report 185, June 1975.

12. At 24 GeV the ratio $\rho^+ / \rho^- = \pi^+ / \pi^- = 1$, see Bonn/Hamburg/Munich Collaboration, paper submitted to European Conference Particle Physics, Budapest, 4-9 July 1977

FIGURE CAPTIONS

Fig.1. The invariant differential cross-section for $pp \to \pi^{\pm}X$, $K^{\pm}X$ at $p_T = 0.75$ GeV, $\sqrt{s} = 45$ GeV versus $x = 2p_L / \sqrt{s}$, compared with the momentum distributions of the appropriate flavours as derived by Field and Feynman (model III ref.8), and with the convoluted distributions $C(q\bar{q},x)$ of eq.(1) and model III; solid lines, Field-Feynman with $xd_{sea}(x) \sim (1-x)^{10}$ (model IIIa) instead of $\sim(1-x)^7$ (model III).

Fig.2. Same as fig.1 for models II of Das et al., ref.7 and Model IIa with $xs(x) = 0.17(1-x)^{10}$.

Fig.3. The invariant differential cross-section for $pp \to \pi^{\pm}X$ at $\sqrt{s} = 45$ GeV in the range $0.55 \leq p_T \leq 1.05$ GeV/c versus $x = 2p_L/\sqrt{s}$ compared with the momentum distributions of the appropriate flavours as derived by Field and Feynman with $xd_{sea}(x) \sim (1-x)^{10}$ (model IIIa) and the convoluted distributions $C(u\bar{d}, x)$ and $C(d\bar{u}, x)$ of eq.1.

Fig.4. The invariant differential cross-section for $pp \to K^{\pm}X$ at $\sqrt{s} = 45$ GeV in the range $0.55 \leq p_T \leq 1.05$ GeV/c versus $x = 2p_L/\sqrt{s}$ compared with the momentum distributions of the appropriate flavours as derived by Field and Feynman with $xd_{sea}(x) \sim (1-x)^{10}$ (model IIIa) and the convoluted distributions $C(u\bar{s}, x)$ and $C(s\bar{u}, x)$.

Fig.5. The π^+ and π^- spectra compared with the convoluted distributions of model III (Field-Feynman) assuming the spectra to contain a 'direct' and a ρ-decay component.

Fig.6. Comparison of the Drell-Yan continuum, computed with the parametrization of models I, II, IIa, III, IIIa and the data of Kaplan et al., ref.10. All models satisfy the sum-rules of eqs.(6) and (7) in the text.

TABLE I

Summary of momentum distributions of the quark flavours in the proton

$$q(x) = q_v(x) + q_s(x)$$

$q_v(x)$ = valence distribution

$q_s(x)$ = sea distribution

Model I (Blankenbecler et al., Duong-Van Ref. 6).

$$u(x) = \frac{0.2(1-x)^7}{x} + 1.89\,\frac{(1-x)^7}{\sqrt{x}} + \begin{cases} 90.2\,x^{3/2}\exp(-7.5\,x) & x < 0.35 \\ 5(1-x)^3 & x \geq 0.35 \end{cases}$$

$$d(x) = \frac{0.2(1-x)^7}{x} + 1.03\,\frac{(1-x)^7}{\sqrt{x}} + 0.7(1-x)\begin{cases} 90.2\,x^{3/2}\exp(-7.5x) & x < 0.35 \\ 5(1-x)^3 & x \geq 0.35 \end{cases}$$

$$\bar{u}(x) = \bar{d}(x) = \bar{s}(x) = s(x) = \frac{0.2(1-x)^7}{x}$$

Model II (Dao et al., Ref. 7).

$$xu_v(x) = 2.99\sqrt{x}(1-x)^4(1 + 5.99\,x - 2.63\sqrt{x})$$
$$xd_v(x) = 1.02\;x(1-x)^5(1.0 + 5.75\,x)$$
$$xs(x) = 0.145\,(1-x)^{11}(1 + 10\,x)$$
$$u_s(x) = \bar{u}_s(x) = d_s(x) = \bar{d}_s(x) = \bar{s}(x) = s(x)$$

Model IIa (This paper).

Derived from model II through Eq.(2) and

$$x\,s(x) = 0.17(1-x)^{10}$$

TABLE I (continued)

Model III (Field and Feynman, Ref. 8).

$$xG(x) = g(x) \sum_{k=0}^{N} (a_k + \sqrt{x} b_k) C_k(x)$$

$$C_k(x) = \cos(k \cos^{-1}(2x-1))$$

$xG(x)$	$xu(x)$	$xd(x)$	$xs(x)$	$x\bar{u}(x)$	$x\bar{d}(x)$	$x\bar{s}(x)$
$g(x)$	$(1-x)^3$	$(x-x)^4$	$(1-x)^8$	$(1-x)^{10}$	$(1-x)^7$	$(1-x)^8$
a_0	161.579	-3.175	0.10	0.17	0.17	0.10
a_1	225.327	-2.937	0.0	0.0	0.0	0.0
a_2	70.699	1.082	0.0	0.0	0.0	0.0
a_3	6.761	0.674	0.0	0.0	0.0	0.0
b_0	-177.909	5.607	0.0	0.0	0.0	0.0
b_1	-230.510	2.6340	0.0	0.0	0.0	0.0
b_2	-52.427	-2.288	0.0	0.0	0.0	0.0
b_3	-1.371	-0.247	0.0	0.0	0.0	0.0

Model IIIa (This paper).

Derived from Model III by the substitutions

$$x\bar{d}(x) = 0.15(1-x)^{10}$$

$$xd(x) \to xd(x) - 0.17(1-x)^7 + 0.15(1-x)^{10}$$

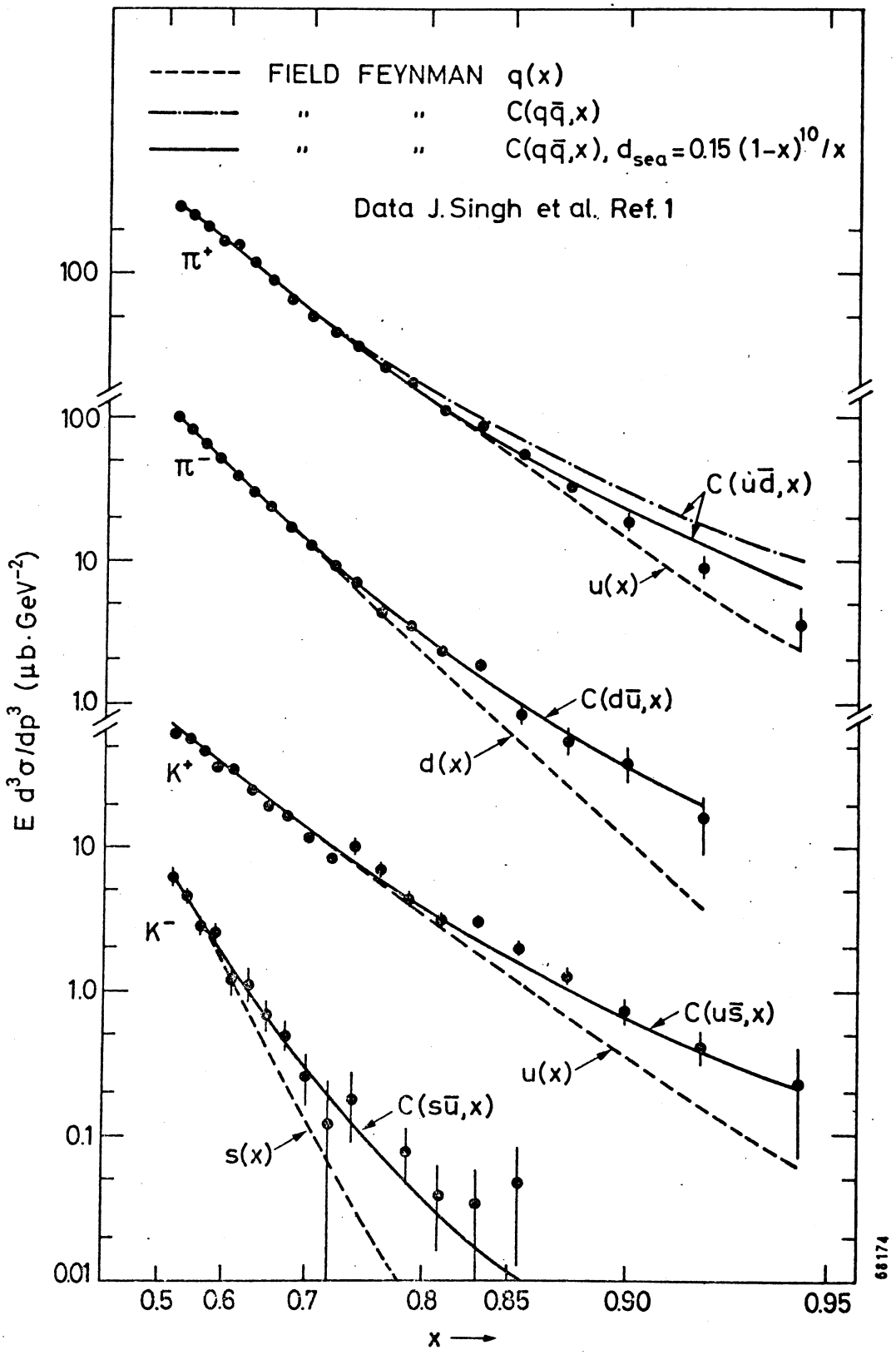
FIELD FEYNMAN q(x)
" " C(qq̄,x)
" " C(qq̄,x), d_sea = 0.15 (1-x)^10 / x
Data J. Singh et al. Ref. 1
π+
π−
K+
K−
C(ūd,x)
u(x)
C(dū,x)
d(x)
C(us̄,x)
u(x)
C(sū,x)
s(x)
E d³σ/dp³ (μb·GeV⁻²)
100
10
1.0
0.1
0.01
0.5
0.6
0.7
0.8
0.85
0.90
0.95
x
68174

Fig.1

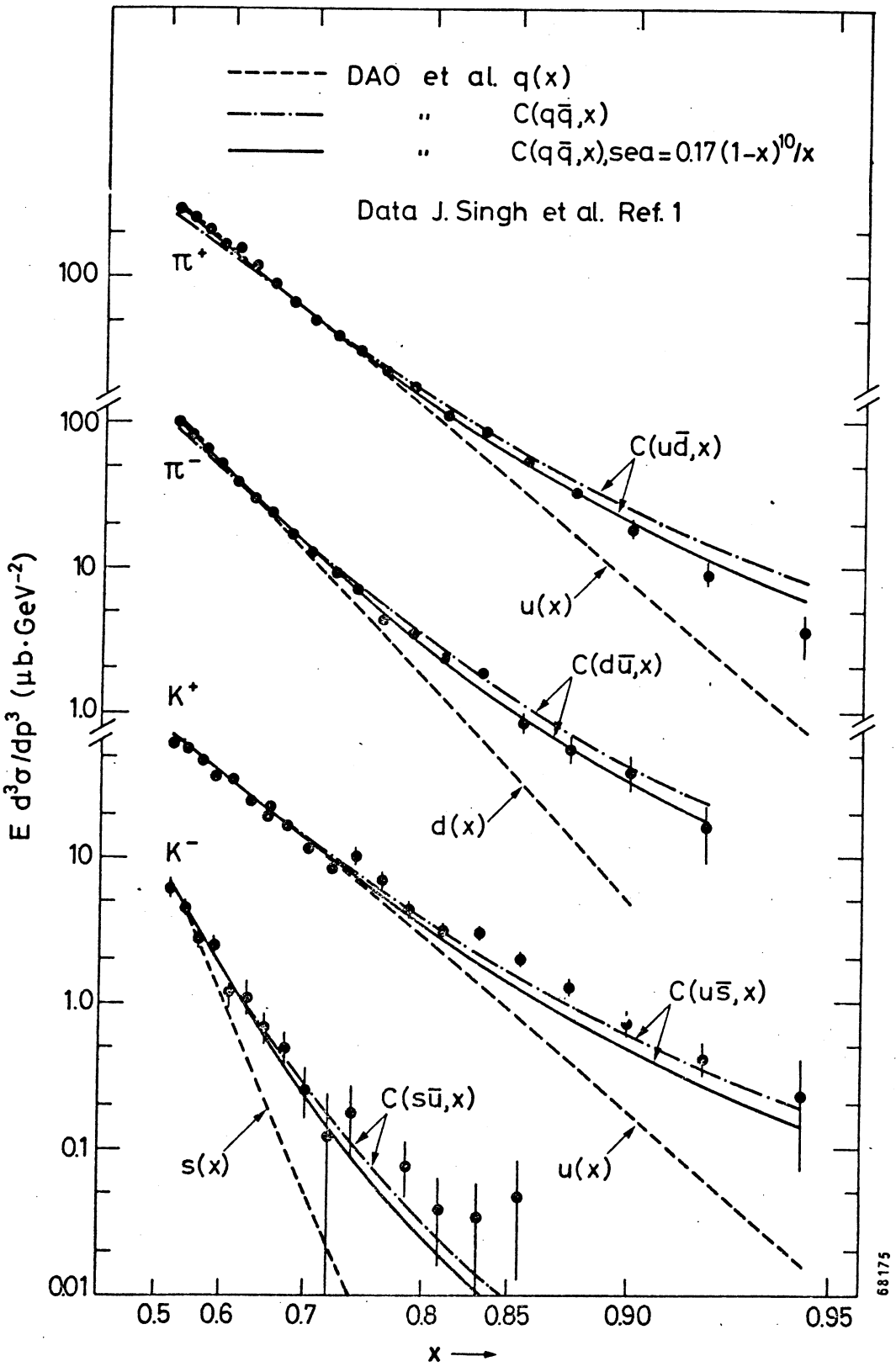
DAO et al. q(x)
" C(qq̄,x)
" C(qq̄,x),sea = 0.17 (1-x)^10/x
Data J. Singh et al. Ref. 1
π+
π−
K+
K−
C(ud̄,x)
u(x)
C(dū,x)
d(x)
C(us̄,x)
C(sū,x)
s(x)
u(x)
E d³σ/dp³ (μb·GeV⁻²)
100
10
1.0
0.1
0.01
0.5
0.6
0.7
0.8
0.85
0.90
0.95
x
68175

Fig.2

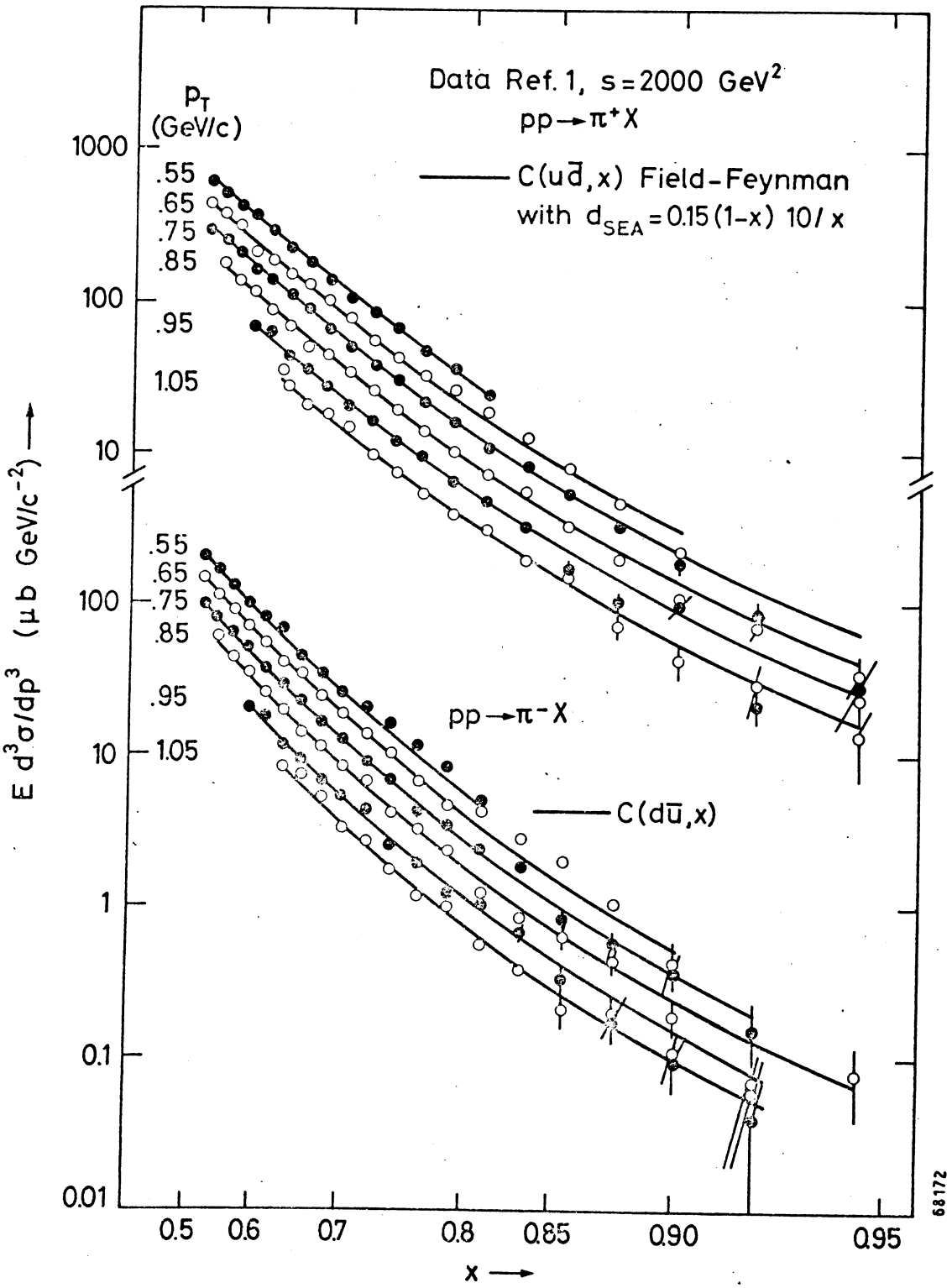
Data Ref. 1, s = 2000 GeV²
pp → π⁺X
C(ud̄, x) Field-Feynman
with d_SEA = 0.15(1-x) 10/x
pp → π⁻X
C(dū, x)
p_T (GeV/c)
.55
.65
.75
.85
.95
1.05
E d³σ/dp³ (μb GeV/c⁻²)
x
1000
100
10
1
0.1
0.01
0.5
0.6
0.7
0.8
0.85
0.90
0.95
68172

Fig.3

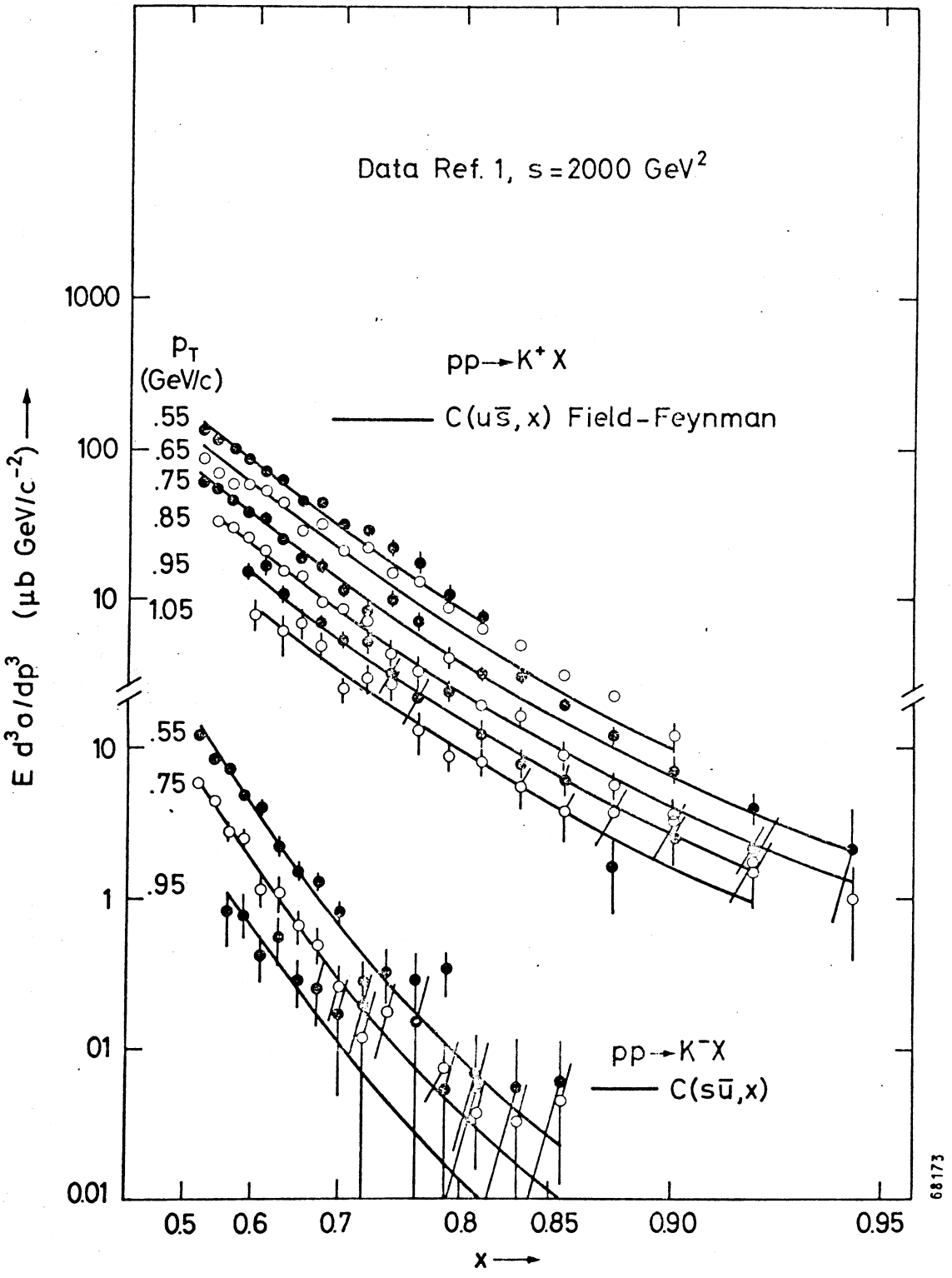
Data Ref. 1, s = 2000 GeV²
pp → K⁺ X
C(us̄, x) Field-Feynman
pp → K⁻X
C(sū, x)
p_T (GeV/c)
.55
.65
.75
.85
.95
1.05
E d³σ/dp³ (μb GeV/c⁻²)
1000
100
10
1
01
0.01
0.5
0.6
0.7
0.8
0.85
0.90
0.95
x
68173

Fig.4

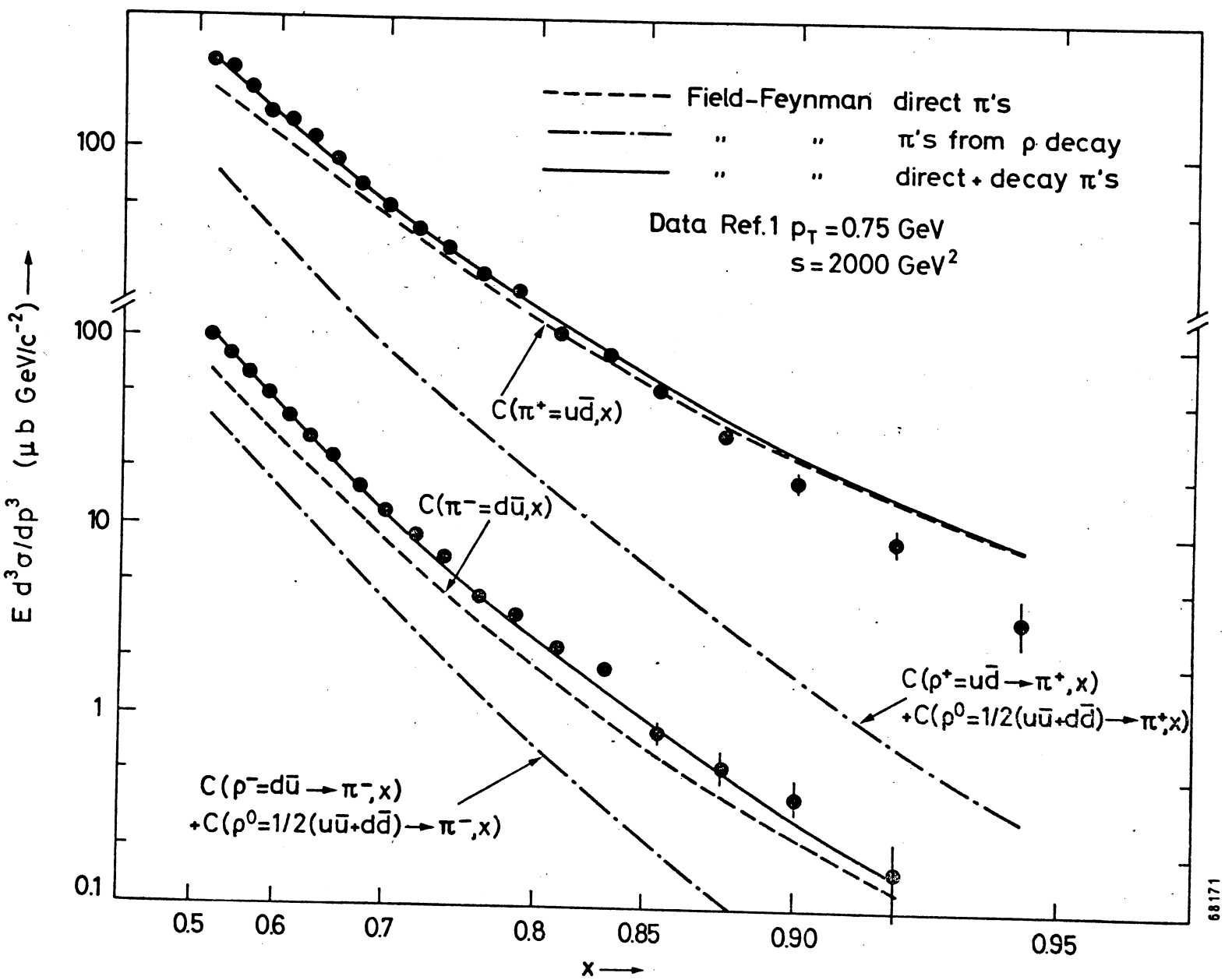
Field-Feynman direct π's
" " π's from ρ decay
" " direct + decay π's
Data Ref.1 p_T = 0.75 GeV
s = 2000 GeV^2
C(π$^+$=ud̄,x)
C(π$^-$=dū,x)
C(ρ$^+$=ud̄ → π$^+$,x)
+C(ρ^0=1/2(uū+dd̄) → π$^+$,x)
C(ρ$^-$=dū → π$^-$,x)
+C(ρ^0=1/2(uū+dd̄) → π$^-$,x)
E d^{3}σ/dp^3 (μb GeV/c^{-2}) →
x →
100
10
1
0.1
0.5
0.6
0.7
0.8
0.85
0.90
0.95
68171

Fig.5

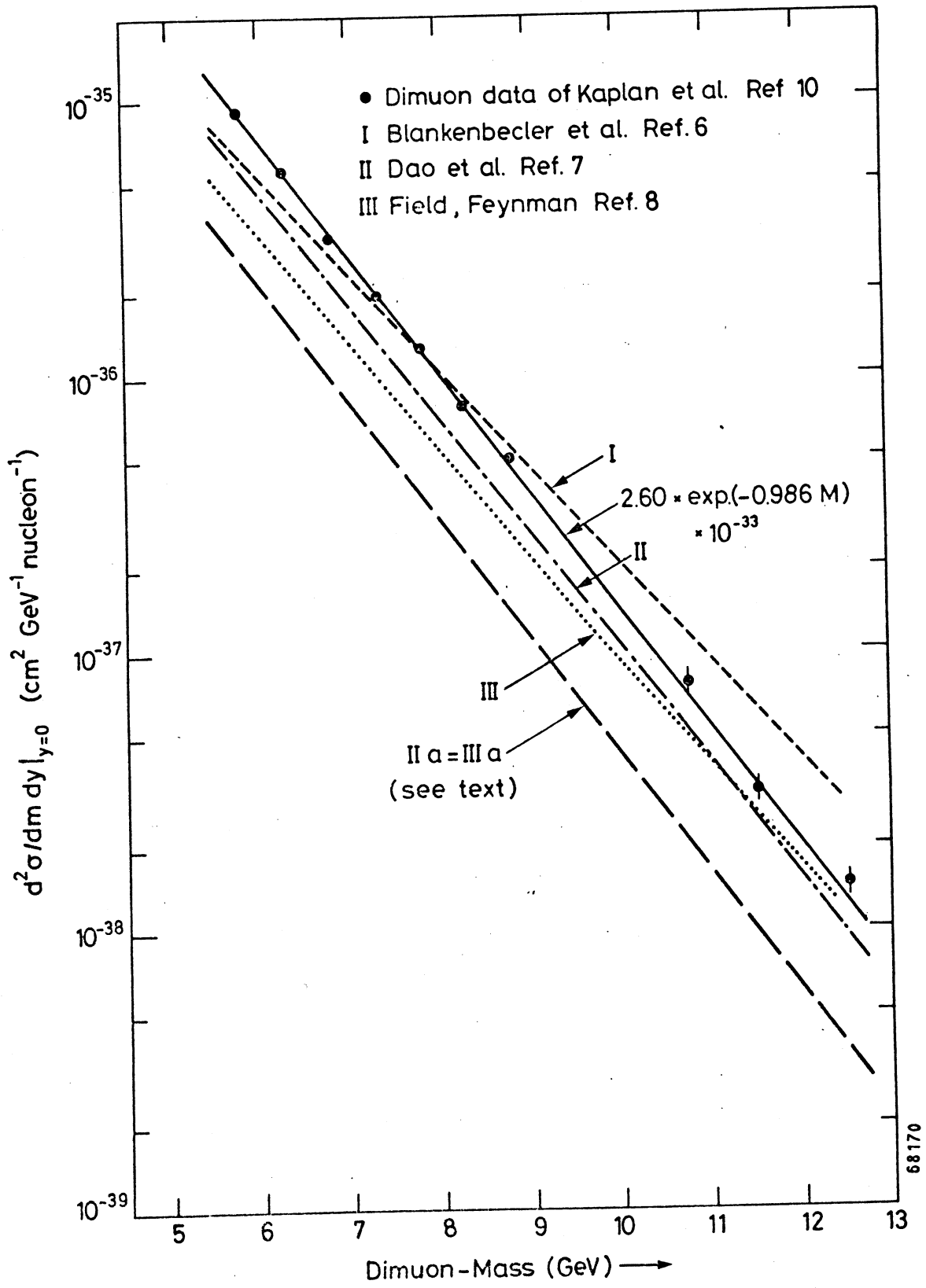
• Dimuon data of Kaplan et al. Ref 10
I Blankenbecler et al. Ref. 6
II Dao et al. Ref. 7
III Field, Feynman Ref. 8
I
2.60 × exp.(-0.986 M)
× 10^-33
II
III
II a = III a
(see text)
10^-35
10^-36
10^-37
10^-38
10^-39
d²σ/dm dy |y=0 (cm² GeV⁻¹ nucleon⁻¹)
5
6
7
8
9
10
11
12
13
Dimuon-Mass (GeV) ⟶
68170

Fig.6